Numerical Experiments on Free-Electron Lasers Without Inversion

Yuri Rostovtsev,[1] Simeon Trendafilov,[1] Alexander Artemiev,[1,3,5] Kishore Kapale,[1]
Gershon Kurizki,[5] and Marlan O. Scully[1,2,4]

[1]*Department of Physics and Institute for Quantum Studies, Texas A&M University, College Station, Texas 77843-4242, USA*
[2]*Department of Electric Engineering, Texas A&M University, College Station, Texas 77843-4242, USA*
[3]*General Physics Institute Russian Academy of Sciences, 38 Vavilov Street, Moscow, 117942, Russia*
[4]*Max-Planck-Institut für Quantenoptik, Hans-Kopfermann-Strasse 1, D-85748, Garching, Germany*
[5]*Chemical Physics Department, Weizmann Institute of Science, Rehovot 76100, Israel*

(Received 23 February 2003; published 30 May 2003)

The inversionless free-electron laser having a drift region consisting of two magnets is analyzed. Performing numerical simulations of electron motion inside wigglers and the drift region, we have shown that this system has a positive mean gain over the entire energy distribution of the electron beam. We study the influence of emittance and the spread of electron energies on the gain.

DOI: 10.1103/PhysRevLett.90.214802 PACS numbers: 41.60.Cr

In a free-electron laser (FEL) [1,2], the accelerated motion of electrons in the "pondermotive potential" of the combined field of the wiggler and the laser produces coherent stimulated radiation. Under the influence of the pondermotive potential, a grating in the spatial density of electrons ("bunching") on the scale of the laser wavelength is produced. As a result net emission is enhanced. FELs are able to produce radiation in widely different frequency domains: from microwaves [3] to x rays [4]. They are used for spectroscopy, laser surgery, material research, and the production intense x-ray beams.

A main limitation on the gain, both for small-gain and large-gain regimes, is set by the spread in the longitudinal momentum of the electrons in the beam. For this reason, much effort has been devoted to producing highly monoenergetic electron beams [5].

Recently, new approaches to increasing the gain in atomic lasers, based on coherence and interference, have been the subject of investigation [6]. This concept has interesting implications for the free-electron laser without inversion (FELWI) as well, even though it is a purely classical rather than quantum device [7].

The FELWI is conceptually implemented via interference of the radiation from two wigglers and an appropriate phasing of the electrons in the drift region between the wigglers [8–11] (shown in Fig. 1). Let us note here that an optical klystron also utilizes a two-stage setup [12], which allows one to increase the maximum gain, but the average gain is zero. The important difference between these two concepts is that the drift region of the FELWI and the dispersion region of the optical klystron have significantly different phase-shift functions.

It was shown that a FELWI requires a correlation between the electron energy change in the first wiggler and the transverse electron velocity [13,14]. A noncollinear FEL geometry provides this correlation and allows for the essentially two-dimensional electron dynamics in the drift region, which is needed for the FELWI phase control [15,16]. It was shown that the FELWI is consistent with Liouville's theorem as well as the generalized Madey's theorem [15]. However, it has not been clear from Refs. [13–15] that a realistic drift region can produce the phase shifts to implement FELWI.

In this Letter we report the results of numerical experiments which have been performed by using a drift region consisting of two bending magnets (defocusing TM_1 and focusing TM_2) as shown in Fig. 1. Simulating the motion of electrons in the wigglers and in the drift region, we find the gain dependence on the energy of the electrons which is depicted in Fig. 2(a) and represents the main result of the paper. It is clear that the average FELWI gain is positive in contrast with an ordinary FEL [Fig. 2(c)] or an optical klystron (OK) which is obtained by removing the bending magnets from the drift region and adjusting the wigglers in a linear configuration [Fig. 2(b)]. The gain for FEL and OK is positive for some energies and negative for other energies, and the average gain over energy is zero. Let us note here that for the ordinary FEL the electron beam should have higher energy than the resonant energy to have gain, and this may be viewed as the inversion condition for the electron beam; in the same sense, the FELWI concept overcomes this condition.

We note also that we consider a small-gain small-signal regime, not a high-gain one. Thus, our numerical simulation allows us to confirm the results of previously published work on this subject [14,15]. In particular, we

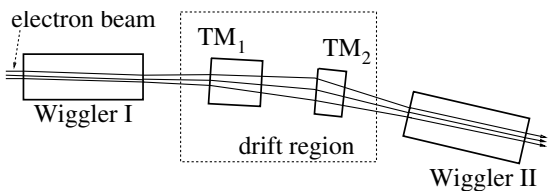

FIG. 1. A FELWI setup.

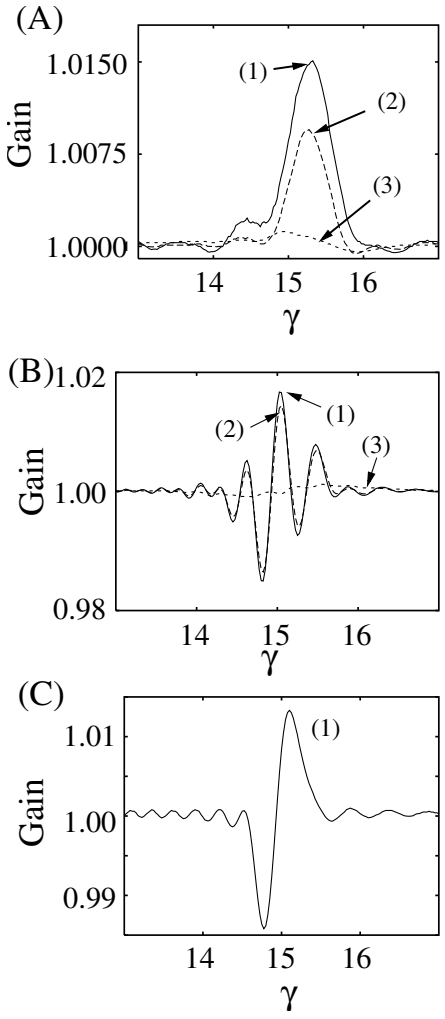

FIG. 2. Gain dependences on electron beam energy with different beam emittances. Plots (a) are obtained for FELWI; (b) for OK; (c) for FEL. Curves (*1*), (*2*), and (*3*) correspond to emittances $\epsilon_{(1)} = 10^{-2}\epsilon_0$, $\epsilon_{(2)} = 10^{-1}\epsilon_0$, $\epsilon_{(3)} = \epsilon_0$ correspondingly, where $\epsilon_0 = 2\pi \times 10^{-6}$ mrad is the emittance of the electron beam available at the Synchrotron Light Source Accelerator in Armenia [17].

demonstrate that the gain in a FELWI for an electron beam having a broad spread of energies is 2 orders of magnitude larger than that for ordinary FELs, and, consequently, one can use much weaker electron beams to obtain lasing.

We solve the FEL equations of motion with z as the independent variable and the longitudinal motion described in terms of the slow phase ψ and the relativistic factor γ. The electromagnetic fields are given by

$$\vec{A}_L = \frac{\vec{e}_y}{\sqrt{2}} A_L e^{i(k_L z - \nu_L t + \psi_0)} + \text{c.c.}, \tag{1}$$

$$\vec{A}_W = \frac{\vec{e}_y}{\sqrt{2}} B_W e^{i(k_W z)} + \text{c.c.}, \tag{2}$$

where $k_L = (2\pi/\lambda_L)$ and ν_L are the wave vector and the frequency of the laser field, respectively, and $k_W = (2\pi/\lambda_W)$ is the wave number of the wiggler field. The Hamiltonian is given by

$$H = \gamma(k_W + k_L) - \frac{\nu_L}{c}(\gamma^2 - 1 - (\vec{p} - e\vec{A})^2)^{1/2}, \tag{3}$$

and it leads to the following equations of electron motion averaged over the wiggler period:

$$\frac{d\gamma}{dz} = -k_L \frac{a_W \tilde{a}_L f_B}{\gamma} \sin\Psi, \tag{4}$$

$$\frac{d\psi}{dz} = k_W - k_L \frac{1 + p_x^2 + p_y^2 + a_W^2 - 2a_W \tilde{a}_L f_B \cos\Psi}{2\gamma^2}, \tag{5}$$

$$\frac{dp_x}{dz} = -\frac{1}{2\gamma}\frac{\partial}{\partial x} a_W^2, \qquad \frac{dp_y}{dz} = -\frac{1}{2\gamma}\frac{\partial}{\partial y} a_W^2, \tag{6}$$

$$\frac{dx}{dz} = \frac{p_x}{\gamma}, \qquad \frac{dy}{dz} = \frac{p_y}{\gamma}, \tag{7}$$

where

$$a_L = \frac{eA_L}{mc}, \qquad a_W = \frac{eB_W}{mck_W}, \tag{8}$$

and $a_L = \tilde{a}_L e^{i\phi_L}$, $\psi = (k_L + k_W)z - \nu_L t + \psi_0$, $\Psi = \psi + \phi_L$, and f_B is the coefficient depending on the type of wiggler. The field equation, in the paraxial and the slowly varying envelope approximation, is given by

$$\left[\frac{\partial}{\partial z} + \frac{1}{2ik_L}\nabla_\perp^2\right]\tilde{a}_L e^{i\phi_L} = ig \sum_{j=1}^{N} \delta(x - x_j)\delta(y - y_j) \times \frac{a_W e^{-i\psi_j}}{\gamma_j}, \tag{9}$$

where

$$g = \frac{ez_0}{mc^2}\frac{f_B}{2k_L}\frac{I}{N}$$

is the coupling constant describing the interaction between the laser field and the electrons; here z_0 is the vacuum impedance, and I is the electron beam current.

To solve the above set of equations numerically, we utilize the FEL numerical simulation code TDA3D [18]. The electron dynamics as dealt with by the code is fully three dimensional. The radiation field however is assumed to have radial symmetry, i.e., $a_L = \tilde{a}_L(r, z)e^{i\phi_L(r,z)}$. The initial conditions for the simulation are specified by the six-dimensional phase-space distribution function $F(\gamma, \Psi, p_x, x, p_y, y)$ at the entrance to the wiggler (at $z = 0$). This distribution is assumed to factorize as $F(\gamma, \Psi, p_x, x, p_y, y) = F_\gamma(\gamma)F_\Psi(\Psi)F_t(p_x, x, p_y, y)$, where F_γ and F_t are usually taken to have Gaussian profiles, and the phase distribution F_Ψ is uniform. The loading of N particles is done using Halton sequences with different prime number bases.

First, to confirm that the results of Refs. [14,15] are correct, it will be instructive to use the program TDA3D, to reproduce the gain of FEL, 1D-FELWI, and FELWI by introducing phase shifts, similar to the ones suggested in Ref. [15]. Namely, introducing the relative detuning $\Omega = (\gamma - \gamma_r)/\gamma_r$ as the difference of electron energy from resonant energy (Ω_0 is the detuning at the entrance of the first wiggler) we can express the phase shift leading to the cancellation of absorption for the electrons having $\Omega_0 < 0$ and to positive gain for $\Omega_0 > 0$ [8]:

$$\Delta\phi = \begin{cases} \pi - \alpha\Omega, & \Omega_0 < 0, \\ -\alpha\Omega, & \Omega_0 > 0, \end{cases} \tag{10}$$

where α is a parameter characterizing the dispersion of the drift region. The gain curve obtained and presented in Fig. 3(a) shows that the average gain is positive for this phase shift. To gain insight into the physics, the phase-space motion studied in [15] demonstrates the way to achieve this cancellation. Namely, adding π to the phase of the appropriate electrons in the drift region reverses their dynamics and removes absorption as a result.

We note that the realization of the phase shift (10) is not a trivial task, because of its dependence on the entrance detuning. As it has been shown in [14,15] this can be achieved by oblique propagation of the laser field with respect to the electron beam (the two-dimensional motion allows one to determine the initial detuning).

It is easier to design a drift region which can introduce the phase shift in the form

$$\Delta\phi = \begin{cases} \pi - \alpha\Omega, & \Omega < 0, \\ -\alpha\Omega, & \Omega > 0. \end{cases} \tag{11}$$

This phase shift also removes the absorption for negative detunings and retains gain for positive detunings, but it causes a larger peak of absorption close to the zero detuning [see Fig. 3(b)]. It appears due to significant bunching of the electrons (see [15] for details) and, finally, the average gain for this case is zero in accordance with either Liouville's or Madey's theorems.

Thus, we reproduce the old results of Refs. [14,15] by using this more sophisticated program, and then, we augment the program in order to simulate the motion of electrons in the drift region. The simulation of the drift region has been accomplished using standard methods of electron beam optics [19]. At the end of the first wiggler, the phase-space variables of TDA3D are converted to the customary coordinates used in describing charged particle beams [19]. The reference trajectory is taken to be that of a resonance energy electron propagating along the wiggler axis. Then the electron trajectories are traced through the drift region with the appropriate first order transfer matrices for the magnetic components utilized in the drift region construction. At the exit to the drift region we revert to the TDA3D variables and restart TDA3D to compute the effect of the second wiggler.

To implement FELWI, we suggest constructing a drift region that consists of two inhomogeneous magnets TM_1 and TM_2. The first one, TM_1, is a defocusing magnet with a B field in the y direction $B_{1y} = 0.9 \times 10^{-2}$ T and an inhomogeneity parameter

$$N_1 = -\frac{1}{h_1 B_{1y}} \left(\frac{dB_{1y}}{dx}\right)\Bigg|_{x=0,y=0} = 3.2,$$

where $h_1 = 1/\rho_1$, ρ_1 being the radius of curvature of the reference electron trajectory through the magnet. The second magnet, TM_2, is focusing with $B_{2y} = 1.8 \times 10^{-2}$ T and

$$N_2 = -\frac{1}{h_2 B_{2y}} \left(\frac{dB_{2y}}{dx}\right)\Bigg|_{x=0,y=0} = -1.96.$$

The length of the first magnet is $L_{TM_1} = 0.25$ m and that of the second is $L_{TM_2} = 0.05$ m. The relevant distances among them and the wigglers (shown in Fig. 1) are as follows: First wiggler to first magnet $L_{W1TM_1} = 0.17$ m; first magnet to second magnet $L_{TM_1TM_2} = 0.05$ m; second magnet to second wiggler $L_{TM_2W2} = 0.05$ m.

Our simulations have been carried out with the following set of realistic electron beam and wiggler parameters that are sufficiently close to experimental situations [17]: electron energy $E = 29.35$ MeV ($\gamma = 15.0$), emittance up to $\epsilon = 2\pi \times 10^{-6}$ m rad, rms beam radius $r = 70$ μm, laser wavelength $\lambda_L = 359$ μm, period of the wiggler magnets $\lambda_W = 2.73$ cm, number of magnets per section $N = 32$, normalized wiggler field $k = (e/mc)(B_{\max}/k_W) = 1.27$, angle between laser and

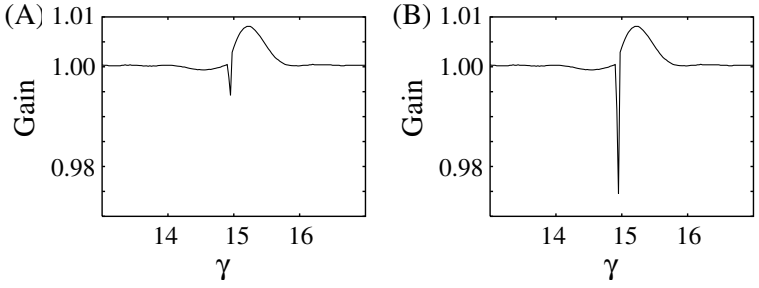

FIG. 3. Gain dependences on electron beam energy (a) for the drift region given by Eq. (10) and (b) for the drift region given by Eq. (11).

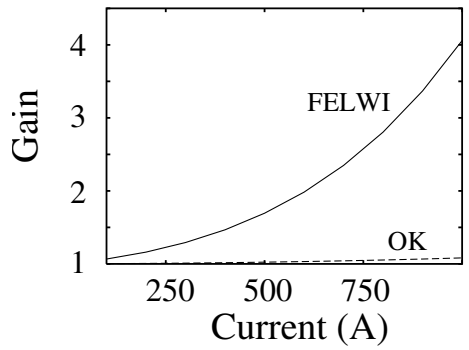

FIG. 4. Gain dependence of FELWI and OK on electron current; emittance is $2\pi \times 10^{-6}$ m rad.

electron beam $\alpha = 0.13$ rad ($\alpha = 7.6°$). The laser beam is directed along the wiggler axis.

We have carefully adjusted the drift region parameters to find the regime which has the positive average gain. This small-gain small-signal regime can be referred to as FELWI and the gain curve is presented in Fig. 2(a). This is the main result of the paper: we demonstrate the positive average gain of the system shown in Fig. 1. Thus, we have proven the validity of the FELWI concept by direct simulations of electron dynamics inside wigglers and the drift region. Note that it is qualitatively different from the approach developed in Ref. [15], where the effect of the drift region has been taken into account by the phase shifts. The finite emittance of the electron beam has not been taken into account in [13,14,15,20].

The next goal is to demonstrate the tolerance of the FELWI gain to the electron beam energy spread. For this $\delta\gamma$ has been taken to be extremely large, namely, $\delta\gamma = 2.0$ while the emittance is $\epsilon = 2\pi \times 10^{-6}$ m rad. Simulations have been performed to obtain the dependence of the FELWI gain on the electron beam current. The results are presented in Fig. 4 which shows that the gain (i.e., the threshold for lasing) is about 2 orders of magnitude larger than that for ordinary FEL.

Thus, we have found the parameters, such that FELWI operation occurs, and studied the gain properties of a new system, for example, its dependence on the emittance, energy spread, and electron beam current. This allows one to study the FELWI in high gain with both small-signal and large-signal regimes, a possibility to obtain short-wavelength lasing, harmonic generations, etc. This study is in progress and the results will be published elsewhere.

In conclusion, we have shown that using a two-stage setup of free-electron lasers with the drift region between them consisting of two bending magnets allows one to obtain the gain which has a positive average value over the electron energies. Using parameters of the electron beam close to the existing experimental setups, we have performed numerical experiments showing that the threshold of such a laser is much lower for the FELWI configuration than for the usual configuration.

The authors gratefully acknowledge very fruitful discussions with Sandra G. Biedron, Jonathan S. Wurtele, and Max Zolotorev, as well as support from the DARPA, the Office of Naval Research, the Texas Advanced Research and Technology Programs, and the U.S.–Israel BSF.

[1] J. M. J. Madey, Nuovo Cimento Soc. Ital. Fis. **50B**, 64 (1979).
[2] C. A. Brau, *Free-Electron Lasers* (Academic, Boston, 1990).
[3] A. Doria, V. B. Asgekar, D. Esposito, *et al.*, Nucl. Instrum. Methods Phys. Res., Sect. A **475**, 296 (2001).
[4] W. B. Colson, Nucl. Instrum. Methods Phys. Res., Sect. A **475**, 397 (2001).
[5] A. M. Sessler, D. H. Whittum, and L. H. Yu, Phys. Rev. Lett. **68**, 309–312 (1992)
[6] O. A. Kocharovskaya and Ya. I. Khanin, Pis'ma Zh. Eksp. Teor. Fiz. **48**, 581 (1988) [JETP Lett. **48**, 630 (1988)]; S. E. Harris, Phys. Rev. Lett. **62**, 1033 (1989); M. O. Scully, S.-Y. Zhu, and A. Gavrielides, Phys. Rev. Lett. **62**, 2813 (1989).
[7] F. A. Hopf, P. Meystre, M. O. Scully, and W. H. Louisell, Phys. Rev. Lett. **37**, 1215 (1976).
[8] D. Nikonov, G. Kurizki, and Yu. Rostovtsev, in *The Wiley Encyclopedia of Electrical and Electronics Engineering* (Wiley, New York, 1999), p. 716.
[9] G. Kurizki, M. O. Scully, and C. Keitel, Phys. Rev. Lett. **70**, 1433 (1993).
[10] B. Sherman, G. Kurizki, D. E. Nikonov, and M. O. Scully, Phys. Rev. Lett. **75**, 4602 (1995).
[11] M. O. Scully *et al.*, Philos. Trans. R. Soc. London, Ser. A **355**, 2305 (1997).
[12] N. A. Vinokurov, in *Proceedings of the 10th International Conference on High Energy Particle Accelerators, Serpukhov, 1977* (Institute of Nuclear Physics, Siberian Branch, USSR Academy of Sciences, Novosibirsk, 1977).
[13] D. E. Nikonov, B. Sherman, G. Kurizki, and M. O. Scully, Opt. Commun. **123**, 363 (1996).
[14] D. E. Nikonov, M. O. Scully, and G. Kurizki, Phys. Rev. E **54**, 6780 (1996).
[15] D. E. Nikonov, Y.V. Rostovtsev, and G. Sussmann, Phys. Rev. E **57**, 3444 (1998).
[16] A. I. Artemiev, M.V. Fedorov, Y.V. Rostovtsev, G. Kurizki, and M. O. Scully, Phys. Rev. Lett. **85**, 4510–4513 (2000).
[17] http://sbfel3.ucsb.edu/www/vl_fel.html, http://www-hasylab.desy.de/facility/fel/, http://www.vanderbilt.edu/fel/.
[18] P. Jha and J. S. Wurtele, Nucl. Instrum. Methods Phys. Res., Sect. A **331**, 477 (1993); T.-M. Tran and J. S. Wurtele, Comput. Phys. Commun. **54**, 263 (1989).
[19] David C. Carey, *The Optics of Charged Particle Beams* (Harwood Academic Publishers, Chur, Switzerland, 1987).
[20] Y.V. Rostovtsev, G. Kurizki, and M. O. Scully, Phys. Rev. E **64**, 026501 (2001).